HEAT FLOW IN A GLULAM JOIST WITH A GLUED-IN STEEL ROD SUBJECTED TO VARIABLE AMBIENT TEMPERATURE

WÄRMEFLUß IN EINEM BRETTSCHICHTHOLZTRÄGER MIT EINER EINGEKLEBTEN STAHLSTANGE BEI VERÄNDERLICHEN TEMPERATUREINWIRKUNGEN

FLUX DE TEMPERATURE DANS UNE POUTRE DU LAMELLE COLLE AVEC UNE GOUJON COLLE SOUMIS AUX TEMPERATURES AMBIENTES VARIABLES

Simon Aicher, Michael Wolf, Gerhard Dill-Langer

SUMMARY

It ist reported on some experimental and numerical investigations concerning temperature distributions in a glulam joist with a protruding axially glued-in threaded steel rod subjected to variable ambient temperatures. The temperature evolution in the two specimens investigated was monitored by thermo-elements attached to the rod along anchorage length and in the wood. In detail, the thermo-elements were placed in the interior of the rod along an axial groove. The groove had been planed into two rods of half circle cross-section which were glued together subsequently. The temperature load over a period of six hours consisted of three intervalls each lasting two hours of warming up, steady state and cooling with temperatures between 20 and 50°C. The measurements revealed significant temperature gradients along anchorage length being more pronounced for the rod with the higher slenderness ratio $\lambda = 20$. The transient numerical simulation was performed in an approximation with an axial-symmetric finite element model. The effective thermal diffusivity of a specifically introduced steel thread/adhesive layer showed the highest sensitivity for fitting the numerical results to the empirical temperatures. Within the frame of the chosen approach a very good agreement of experimental and theoretical data was obtained.

ZUSAMMENFASSUNG

Es wird über erste experimentelle und numerische Untersuchungen zu Temperaturverteilungen in einem Brettschichtholzträger mit einer stirnseitig hervorstehenden axial eingeklebten Stahlgewindestange bei Beanspruchung durch veränderliche Außentemperaturen berichtet. Die Temperatur-entwicklung in den beiden untersuchten Prüfkörpern wurde durch Thermoelemente, die an der Gewindestange längs der Einbindelänge und im Holz angebracht waren, registriert. Im Detail betrachtet, wurden die Thermoelemente in einer axialen Nut im Inneren der Stange appliziert. Die Herstellung der innenliegenden Nut erfolgte durch Einfräsen in zwei Gewindestangen mit jeweils halbkreisförmig bearbeitetem Querschnitt, die anschließend verklebt wurden. Die Temperaturbelastung über einen Zeitraum von sechs Stunden bestand aus drei zweistündigen Aufwärme-, Halte- und Abkühlabschnitten mit Temperaturen zwischen 20 und 50°C. Die Messungen ergaben deutliche Temperaturgradienten über die Verankerungslänge, die bei der Stange mit größerem Schlankheitsgrad von $\lambda = 20$ ausgeprägter waren. Die transiente numerische Simulation wurde in einer Näherung mittels eines axialsymmetrischen Finite Element Modells durchgeführt. Die effektive Temperaturleitfähigkeit einer speziell eingeführten Stahlgewinde-Klebstoffschicht zeigte die größte Sensitivität bei der Anpassung der numerischen Ergebnisse an die gemessenen Temperaturen. Im Rahmen des gewählten Ansatzes wurde eine sehr gute Übereinstimmung zwischen den experimentellen und theoretischen Ergebnissen erhalten.

RESUME

Il est rapporté des premières investigations experimentelles et numériques aux distributions de température dans du lamellé-collé avec une tige filetée resortant de la section transversale soumis a une température ambiente variable. L’évolution du température dans les deux épreuvettes étudiés était enrégistré par des thermocouples qui étaient montés le long de l’ancrage de tige filetée et dans le bois. En détail, les thermocouples ont été appliqués dans une entaille axiale à l’entérieure du goujon métallique. L’entaille intérieure a été fait par fraisage de deux goujons métalliques demi-circulaires; après les deux parts étaient collés. Le chargement thermique dans une temps de six heures comprenait trois phases de deux heures de l’échauffement, de la température stationaire et de refroidissement avec de températures entre 20 et 50°C. Les mesures montraint des gradients du température le long de l’ancrage qui étaint plus fort en cas d’élancement λ=20. La simulation transitoire numérique était conduite en approximation avec une modélisation par éléments finis axisymmetriques. La conductibilité des élements d'une couche spéciale combinant l'adhesive et le métal a montré la plus grand sensibilité a l'adjustement des résultats numériques et expérimenteaux. Dans le cadre de l'approche choisie on a obtenue une très bonne agréement entre les résultats expérimenteaux et théoretiques.

KEYWORDS: glued-in steel rods, metric thread, glulam, transient heat transfer, variable temperature loads, thermo-elements

1. INTRODUCTION

Glued-in rods in wood resp. glulam represent a very promising connecting method in timber engineering and have already been employed in several large scale constructions outside Germany. Especially in joints where the steel rods are not entirely hidden in the timber but are screwed or welded to connecting devices of steel (i.a. [RIBERHOLT, 1986]; [BUCHANAN AND TOWNSEND, 1990]; [FAIRWEATHER, 1992]; [AICHER ET. AL. 1998]) which are in contact to the ambient air the impact of varying temperatures is of interest. The extremely different thermal conductivities resp. diffusivities of wood and steel obviously lead to time dependant temperature gradients which result in eigenstrains resp. -stresses. Finally the eigenstress state is influenced by a 3 to 5 times higher temperatur elongation coefficient of steel as compared to wood.

A limited number of investigations have been addressed to the stated problem so far; an extensive experimental test program has been carried out by [EHLBECK ET AL., 1992]. In the cited investigations the length of the stepped temperature cycles was two days with a temperature difference of 50°C at different relative humidities of the air. Thermo-elements and strain gauges were mounted in a side groove along the rod axis then filled by an epoxy resin necessitating special attention to delayed temperature hardening of the adhesive at tests with elevated temperatures. Conclusions bound to the investigated temperature cycles state a rather uniform temperature distribution along anchorage length within several hours after the temperature change and hence constant strains.

Theoretical investigations on the transient temperature evolution in the regarded hybrid material joint are not stated in literature. The recent FMPA investigation on the temperature issue described here had essentially two aims:

- to investigate the experimental implications and results with threaded test rods having an interior groove where all measuring devices are applied. This method has been first adopted by [AMSTUTZ, 1955] in investigations on the bond behaviour of deformed steel bars in concrete,
- to make a first attempt of a numerical simulation of the problem.

This paper covers exclusively the temperature evolution aspect; the associated eigenstrain - stress issue will be forwarded seperately.

2. EXPERIMENTAL INVESTIGATIONS

2.1 Specimen built-up

The investigations so far were performed with two glulam specimens No. 1 and 2 with a square cross-section of 160 x 160 mm, incorporating a threaded steel rod glued-in parallel to the fiber direction at one end cross-section. Figure 1 depicts the general built-up of the specimens. The difference of both similar specimens mainly concerned the rod diameter d and the anchorage length l_a, thus the rod slenderness ratio $\lambda_a = l_a / d$. For specimens No. 1 and 2 quantities d, l_a, λ_a were 200, 20, 10 and 320, 16 and 20, respectively. Table 1 contains a compilation of all relevant dimensions. Figures 1b, c reveal the loading conditions of the specimens when mounted into the loading rig. In order to measure the heat flow, the specimens were equipped with thermo-elements mounted to the threaded rods along anchorage length and in the wood. The employed thermo-elements consisted of copper constantan wires, fixed to the rod and wood with epoxy adhesive.

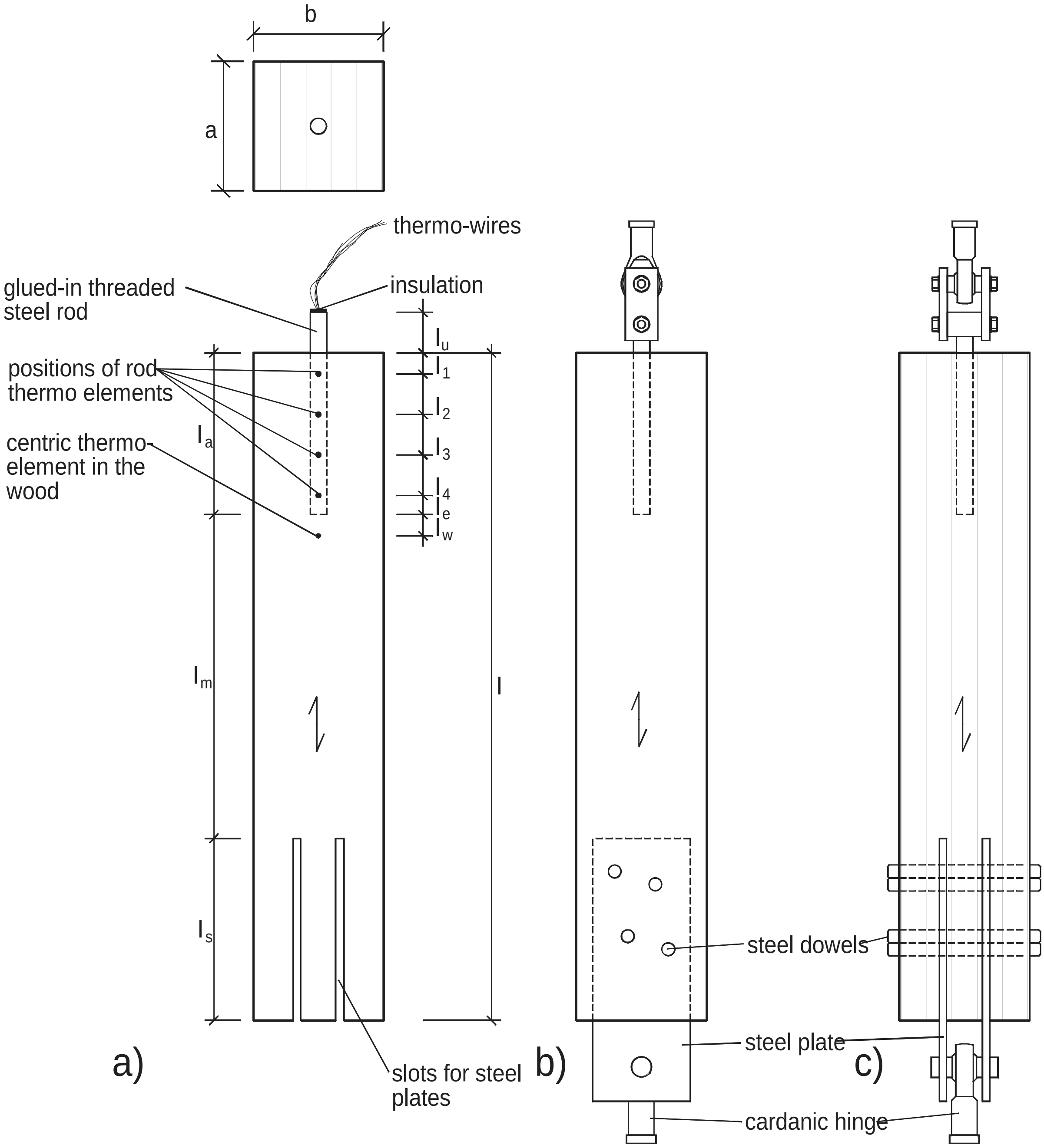

Fig. 1 a-c: *General built-up of investigated specimens No. 1 and 2*

In order to avoid the cited problems in experimental data interpretation experienced by [EHLBECK ET. AL. 1992], it was decided to manufacture test rods which contain all measuring devices - thermo-elements, strain gauges - in an interior axial groove. Figure 2 gives a schematic view of the built-up of the rods and of the application of the thermo-elements.

Dimensions		unit	specimen No 1	specimen No 2
glulam				
cross-section	a x b	mm	160 x 160	160 x 160
total length	l	mm	825	1185
anchorage length	l_a	mm	200	320
intermediate length	l_m	mm	400	640
slot length	l_s	mm	225	225
hole diameter	dh	mm	21	17
steel rod, metric thread				
total length	$l_a + l_u$	mm	200 + 50	320 + 50
nom. diameter	$d = d_{nom}$	mm	20	16
core diameter	d_c	mm	16,8	13,3
slenderness	l_a / d_{nom}	-	10	20
groove cross-section	agr x lgr	mm	6 x 6	4,8 x 4,8
thermo-elements				
along glued-in rod	l_1	mm	30	42
	l_2	mm	46	75
	l_3	mm	46	75
	l_4	mm	46	75
	l_e	mm	32	53
in wood	lw	mm	32	32
substitute dimensions for axial-symmetric analysis				
glulam $\left(a \cdot b = \pi\, d_w^2 / 4\right)$	d_w	mm	180,1	180,1
rod-groove $\left(a_{gr} \cdot b_{gr} = \pi\, d_{gr}^2 / 4\right)$	d_{gr}	mm	6,77	5,41

Table 1: *Dimensions of investigated specimens No. 1 and 2, locations of thermo-elements and substitute dimension for approximate axial-symmetric finite element analysis*

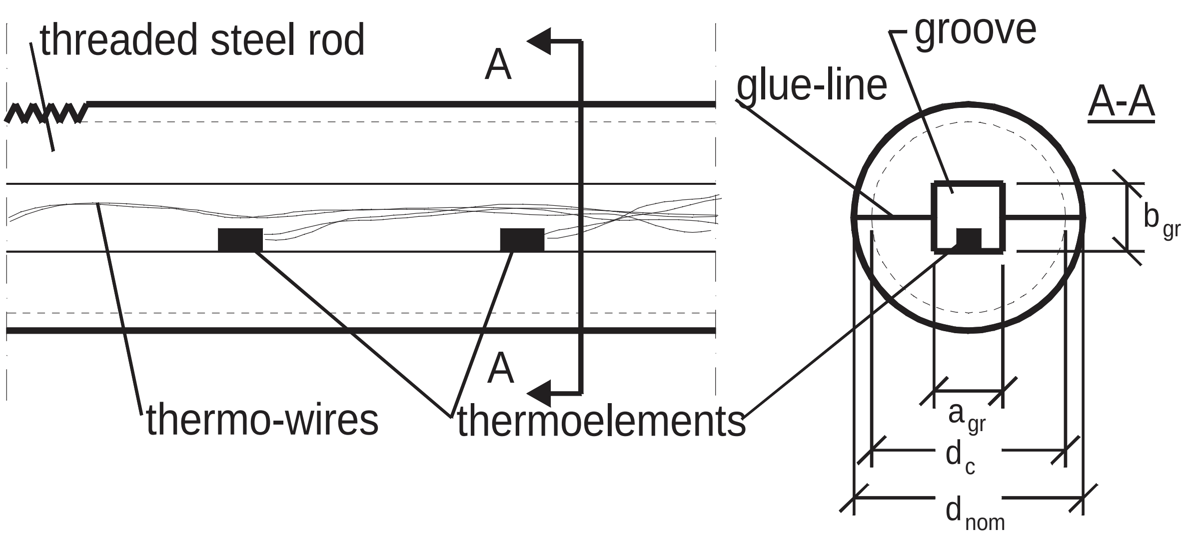

Fig. 2: *Schematic longitudinal- and cross-sectional views of employed threaded steel rods with internally applied thermo-elements*

The manufacturing of the rods was conceived to obtain surfaces of the threaded rods ressembling best possible the periphery of an unprocessed rod. This was achieved for each test rod by planing the cross-sections of two rods to a half circle. Then the rectangular grooves were planed along the axis of both rod halves. After application of the thermo-elements the halves were glued together by means of an epoxy adhesive of low viscosity. The curing of the rod bond took place in clamped conditions at a slightly elevated temperature of 40°C. Both ends of the rods were sealed with air tight isolation material.

When manufacturing a half circle shaped rod by planing away one half of the cross-section of the original rod, the half circle shaped rod tends to bend due to freed eigenstresses which are introduced into the periphery of the rod during cold tensioning. As the eigenstresses and hence the bow increase significantly with higher steel qualities, threaded rods of rather low steel quality of 4.6 were used.

Before bonding the rods into the specimen the functioning of the measuring devices was tested extensively. The adhesive used to bond in the rods was a 2component epoxy (Ciba AW 139 / HV 953 U).

Apart from the thermo-elements applied to the interior of the rod a thermo-element was positioned in the wood in the middle of the cross-section at 20 mm distance from the bonded-in end of the steel rod. The moisture content of the glulam specimens at the time of gluing-in the threaded rods was about 10%.

Figure 3 shows a photograph of one of the specimens with the thermo-wires and the wires of the strain gauges sticking out of the protruding end of the glued-in rod.

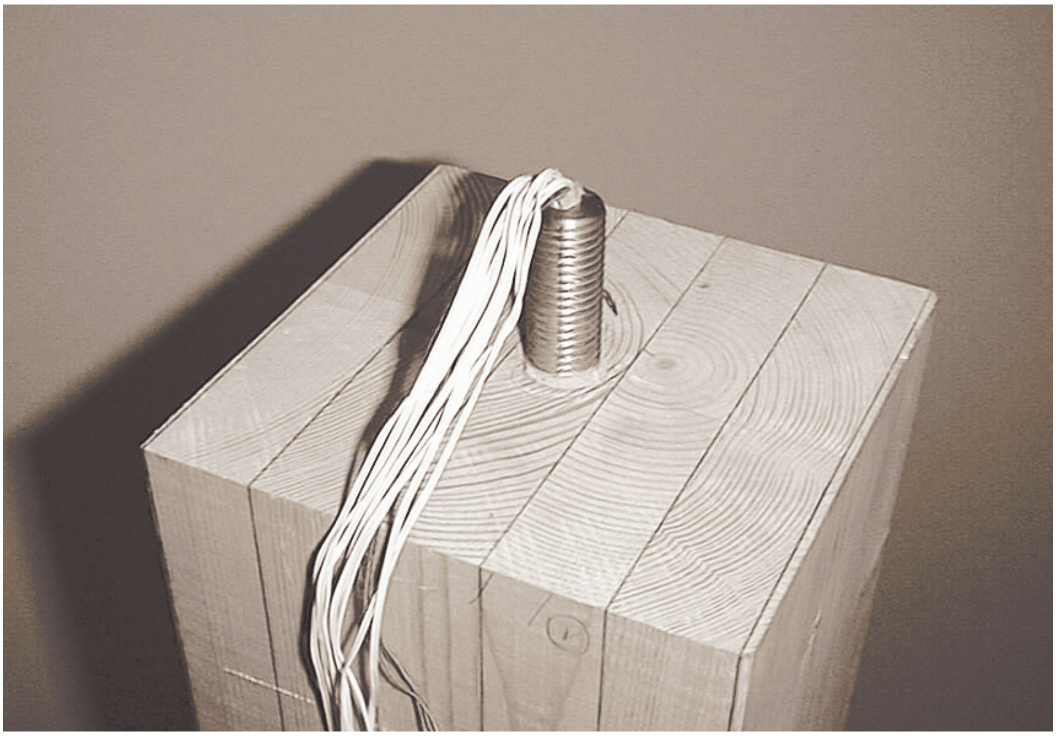

Fig. 3: *Photograph of the end face of specimen No. 1 with the protruding rod end and sticking out thermo- and strain gauge wires*

2.2 Applied temperature load at quasi constant moisture conditions

Climate recordings under roof at FMPA showed that temperatures in summer time may easily vary by about ΔT = 20 to 30°C during one day. Hereby temperatures increase during noon from about 20 - 25°C to 40 - 50°C; the elevated temperatures last for about 1,5 to 3 hours and then gradually decrease. In more Southern European areas the daily temperature differences supposedly may well be 10 to 15°C higher.

The tests conducted so far consisted of a simple temperature cycle, lasting for six hours (Fig. 4). The cycle consists of three stages: a first degressive increase of the ambient temperature from 20 to 50°C in 2 hours, then a 2 hours period of constant temperature of 50 °C and third a degressive cooling phase to 20°C within 2 hours.

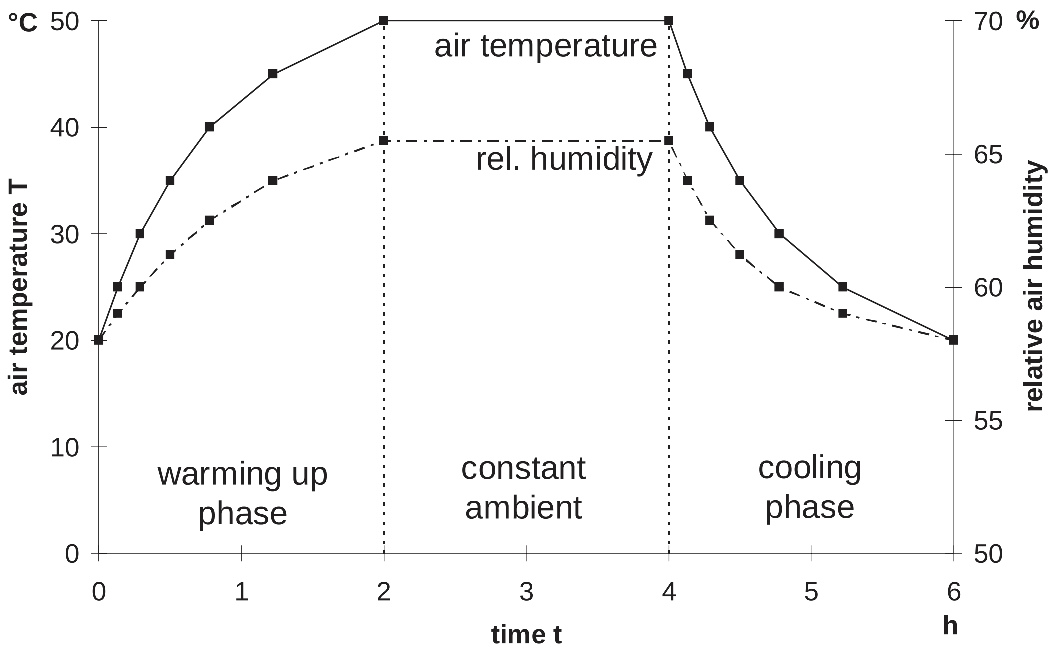

Fig. 4: *Course of applied temperature and relative humidity of ambient air*

Due to the stepwise temperature changes in combination with the crude control mechanism of the climate chamber the temperature course in the warming up phase however was rather linear (see Fig. 10). In order to keep the moisture content of the wood quasi constant during temperature variations the relative humidity of the ambient air of the chamber was adjusted at every temperature change accordingly to maintain a moisture content of the wood of 10%. For the tests the specimens were mounted in vertical position to the test rigs installed in the climate chamber; in the pure temperature test the self weight of the specimens was compensated. All side and end grain faces of the specimens were fully exposed to the ambient air.

2.3 Test results

Figures 5a,b reveal the measured temperature evolutions of both specimens at the locations of the thermo-elements along anchorage length during the heating, steady state and cooling phase.

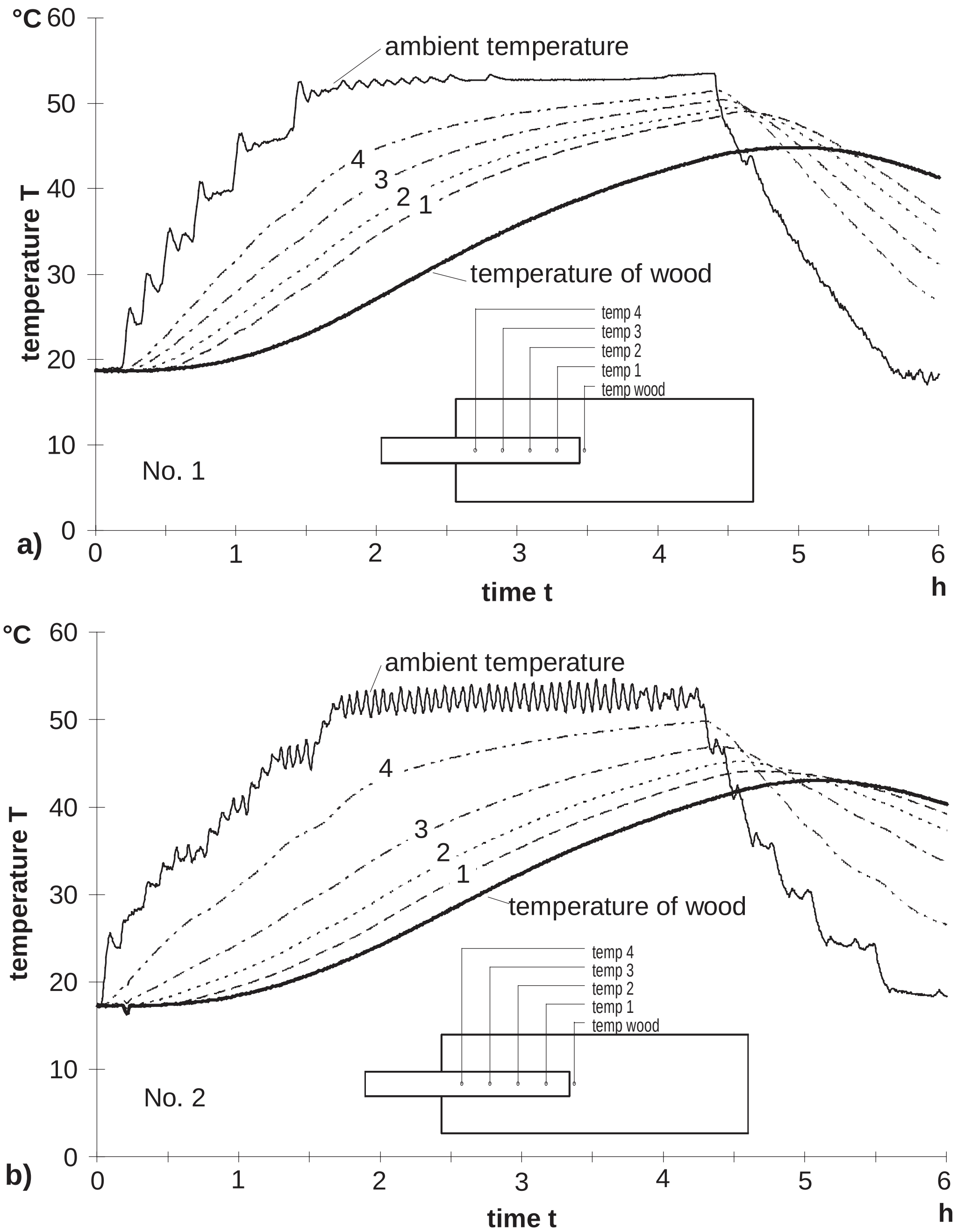

Fig. 5 a-b: *Measured temperatures for specimens No. 1 and No. 2*
a) No. 1 ($l_a/d=10$, $a/d=9$)
b) No. 2 ($l_a/d=20$, $a/d=11.25$)

Both figures show distinct differences of the temperature along the anchorage length of the rod (thermo-elements 1 - 4) and between ambient temperature and the temperature of the wood in the center of the cross-section close to the rod end. It can be seen further that the temperature gradients decrease as anticipated with sustained constant elevated temperature. The temperature gradient along the rod is more pronounced for specimens No. 2 with the higher slenderness ratio of $\lambda = 20$. The absolute differences of the temperatures between the protruding and the embedded end of the rods at the end of the heating period are considerably smaller for specimen No. 1 with $\lambda = 10$ compared to specimen No. 2 with $\lambda = 20$. In the cooling phase the temperature differences are, as anticipated, contrary to the warming up phase. The influence of the slenderness ratio on the rod temperature distribution is revealed in Fig. 6.

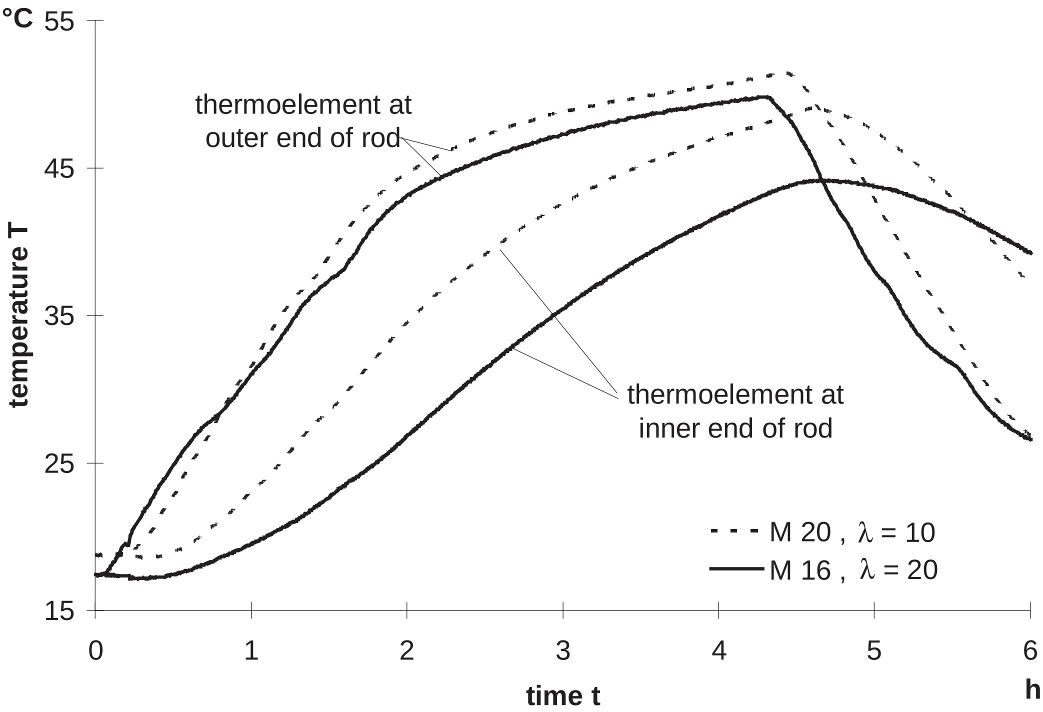

Fig. 6: *Influence of slenderness ratio on the temperature evolution at both ends of the anchorage length*

3. HEAT FLOW ANALYSIS

3.1 Basic equations

The Fourier equation of heat conduction in a cylindrically anisotropic material (rotation axis z here coinciding with the grain direction) is

$$D_{rr}\left[\frac{1}{r}\frac{\partial T}{\partial r}+\frac{\partial^2 T}{\partial r^2}\right]+D_{\varphi\varphi}\frac{1}{r^2}\frac{\partial^2 T}{\partial \varphi^2}+D_{zz}\frac{\partial^2 T}{\partial z^2}=\frac{\partial T(r,\varphi,z,t)}{\partial t} \tag{1}$$

where

T and t			temperature and time,
$D_{ii}=\frac{k_i}{\rho\, C_p}$	$\left[\frac{mm^2}{h}\right]$,	$i=r,\rho,z$	thermal diffusivities,
k_i	$\left[\frac{W}{m\,K}\right]$		thermal conductivities,
C_p	$\left[\frac{Ws}{kgK}\right]$		specific heat,
ρ	$\left[\frac{kg}{m^3}\right]$		mass density.

The boundary condition for the investigated heat conduction problem was assumed to be of the convective type (Newton's law of cooling), so

$$\frac{\partial T}{\partial n}=-\frac{h_n}{k_n}\left(T_s-T_B\right) \tag{2}$$

where

h_n $\left[\frac{W}{m^2K}\right]$ convection heat transfer coefficient in direction n of the outward normal of the boundary

T_s, T_B temperature of the surface resp. of the ambient air.

Symbol ∂/∂_n denotes differentiation in the direction of the outward normal of the boundary surface (here n = z,r). For heat transfer coefficients $h_n \rightarrow \infty$ the boundary condition (2) tends to the situation where the temperature distribution is prescribed at the boundary surface, say is for instance equal to the ambient temperature.

3.2 Modelling details, material properties

The numerical simulation of the temperature evolution in the experimentally investigated specimens was performed by means of finite element analysis (FEA). In an approximation the actual 3D geometry was replaced by an axial symmetric model. Figures 8a,b give the geometry; the dimensional quantities are listed in Table 1. Figure 7 shows the finite element discretization. The model was built by 8 node axial symmetric thermal elements with cylindrical anisotropic thermal conduction capability. The employed thermal element can be replaced by an equivalent structural element performed in a second step of the analysis not discussed here.

It can be seen from Fig. 8 that the simulation model of the actual three component compound – wood/adhesive/steel - contained a fourth ”material” being the thread/adhesive layer primarily used for modelling of the contact conductance of the steel/adhesive interface (see below).

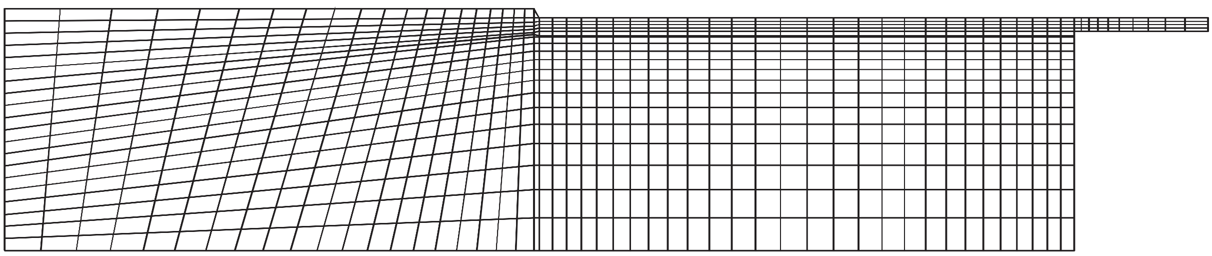

Fig. 7: Finite element mesh of the employed axial-symmetric model

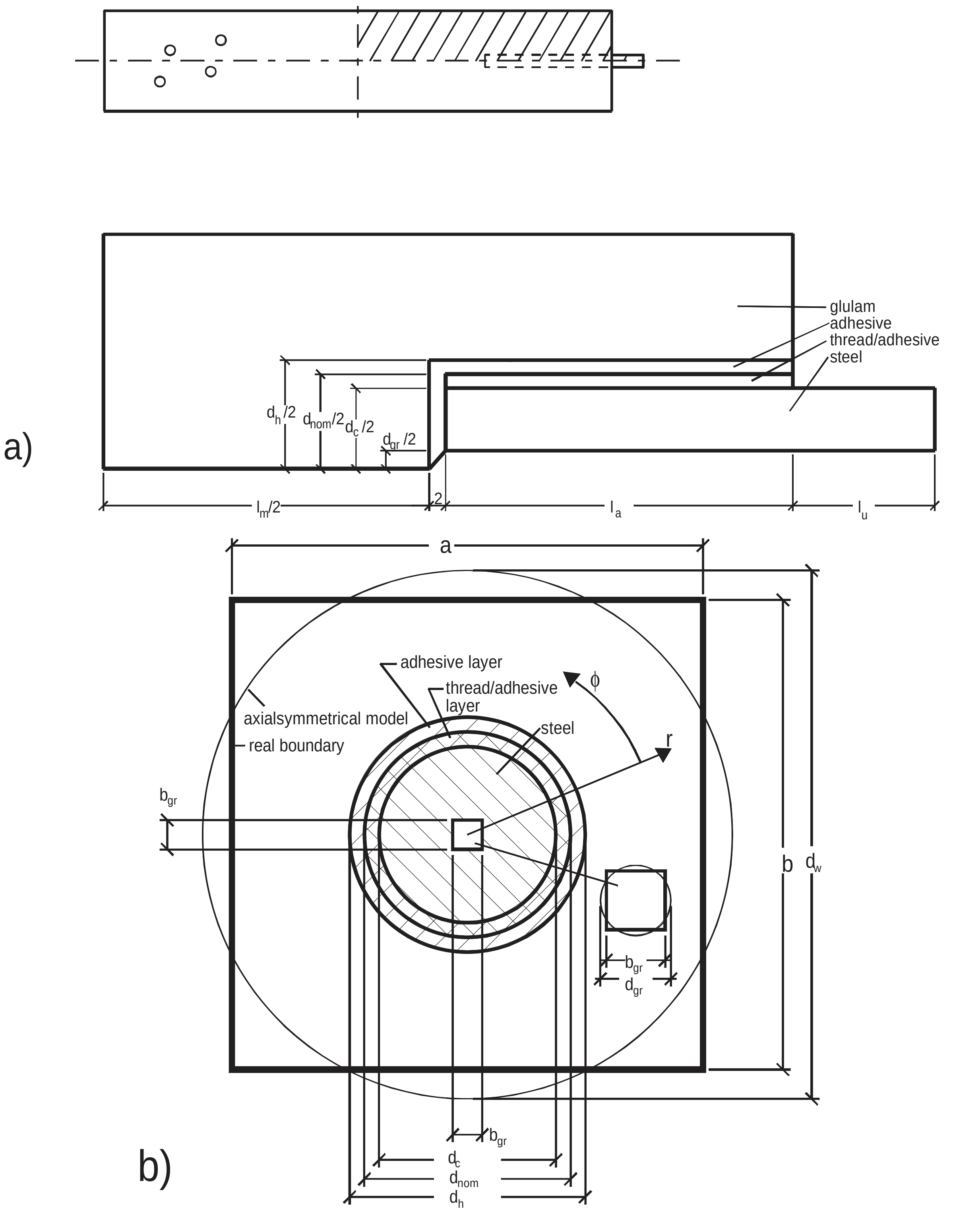

Fig. 8 a-b: Geometry of employed axial-symmetric finite-element model
a) length section b) cross-section

The material properties employed in the thermal analysis are compiled in Table 2.With respect to the thermal material properties, it has to be reminded that the primary aim of the transient temperature modelling was to obtain computational temperature fields which agree best possible with empirical pointwise temperature measurements. The computational temperature fields are applied as loads for the mechanical problem, i.e. for the numerical assessment of the temperature induced eigenstrains and eigenstresses to be compared with test results. For this reason the absolute values of the employed material properties are of secondary interest. Nevertheless mainly literature based properties (thermal conductivities, specific heats) were used. However heat transfer coefficients and the thermal diffusivity of the thread/adhesive layer (see below) were regarded as parameters adjustable in a certain range for the fitting of the analysis to the empirical data.

The specific heat of wood depends pronouncedly on the moisture content u; the quantity given in Table 2 for the specific heat of glulam is based on [KOLLMANN, 1982]

$$C_p(u) = \frac{u + 0{,}324}{1 + u} \cdot 4{,}19 \quad \left[\frac{\text{kJ}}{\text{kg K}}\right] \tag{3}$$

using a moisture content of u = 0,12.

3.3 Issue of contact conductance

At the interface of two materials with different thermal conductivities in general a sudden jump of the temperature profile is encountered unless perfect thermal contact exists and hence continuity of temperature and heat flux. The temperature discontinuity in the interface is due to micro voids filled with air. Similarily to the convection coefficients of the outer boundary of the continuum, contact conductances h_c [W/m^{2}K] should be prescribed for the interior interfaces of the regarded problem, here especially for the interface steel/adhesive. However the employed FE code ANSYS does not enable the input of contact conductances. The problem was solved in such manner that the contact conductance of the steel/adhesive inface was incorporated into the effective thermal diffusivity of the thread/adhesive layer.

		units	wood		steel	adhe-sive	thread/ adhesive layer
			parallel to grain	perpen-dicular to grain			
mass density	ρ	$\frac{kg}{m^3}$	450		7850	1400	4625
thermal conductivity	k	$\frac{W}{m\ K}$	0,29 [1)]	0,13 [1)]	60 [1)]	0,28 [2)]	0,04
specific heat	C_p	$\frac{kJ}{kg\ \ K}$	1,66 [3)]		0,4	1,5 [4)]	1
thermal diffusivity	D	$\frac{mm^2}{h}$	1400	620	68800	480	31,1
(convection) heat transfer coefficient [5)]	h	$\frac{W}{m^2\ K}$	50	25	100	50	50

Table 2: *Compilation of thermal analysis properties of all materials of the investigated specimen built-up.*

[1)] acc. to DIN 4108, part 4 *[2)] acc. to [N.N., 1990]*

[3)] acc. to eq. (3) with u = 0,12 *[4)] acc. to [Batzer, 1985]*

[5)] literature data for forced convection of gas media vary roughly between 10 to 100 W/(m² K) [GRÖBER, 1963]; a value of 25 W/(m² K) is assumed for convection at exterior walls in DIN 4108, part4

Compared to heat transfer coefficients the thermal diffusivity of the thread/adhesive layer revealed to be the most sensitive parameter for adjustment of the theoretical and empirical temperature distribution. A diffusivity value of $D = 31{,}1\ mm^2/h$ gave the best agreement with empirical temperature measurements.

3.4 Results of heat flow analysis

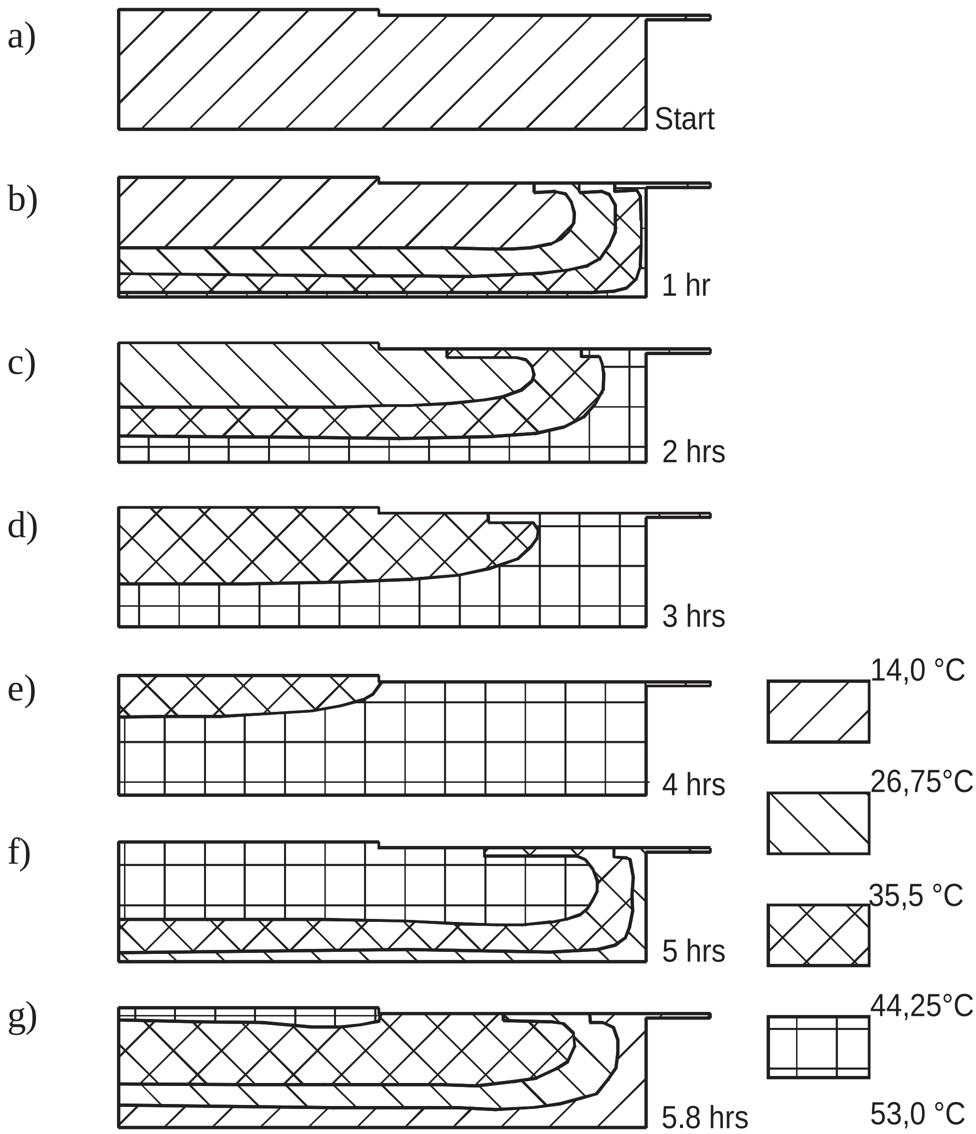

Fig. 9: *Temperature distribution of specimen No. 1 at different times of the applied temperature history*

Figures 9a - g show the spatial evolution of the temperature field in the wood and along the steel rod for different times of the warming up, steady state and cooling phase. The figures reveal a temperature exchange in the wood occuring faster than anticipated.

4. COMPARISON OF EXPERIMENTAL AND MODELLING RESULTS

Figures 10 and 11 depict the high agreement between the experimentally obtained temperature evolution and the numerical analysis. The empirical observation of pronounced temperature gradients along rod length was confirmed by the numerical calculations. Furthermore the results of FE-analysis also revealed the quantitative differences between the transient temperature distributions of the two specimens with different slenderness ratios. With respect to material parameters used in the calculations it shall be reminded that the primary objective of the numerical modelling was the fitting of the measured data.

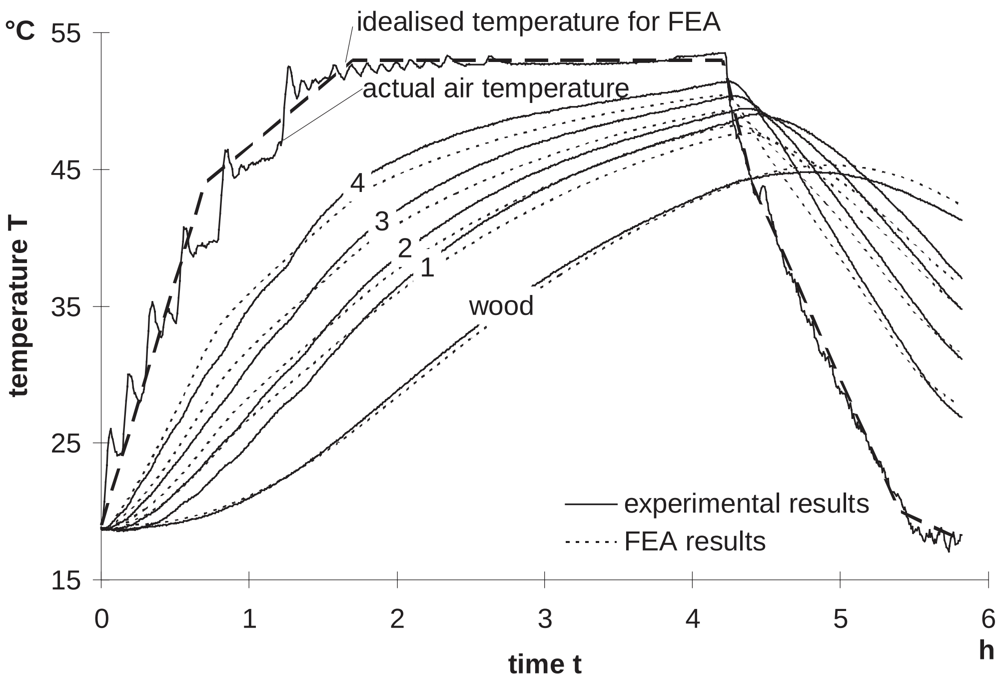

Fig. 10: *Comparison of experimental- and FEA-results in the case of specimen No. 1*

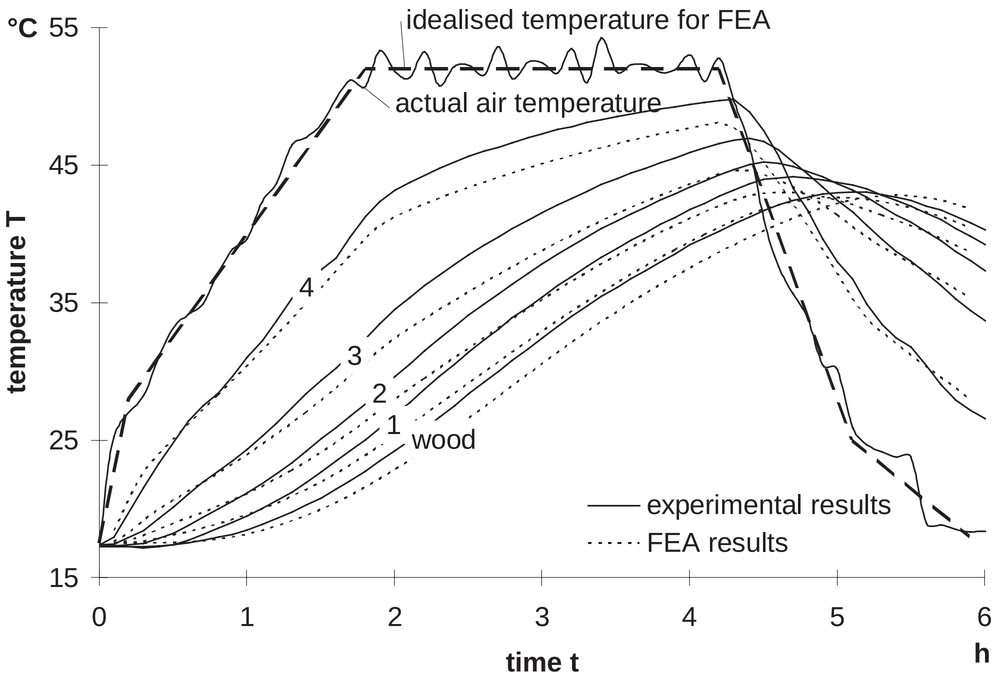

Fig. 11: *Comparison of experimental- and FEA-results in the case of specimen No. 2*

5. CONCLUSIONS

Empirical tests in conjunction with FE-analysis were conducted to investigate the heat conduction problem of a glulam joist with a protruding steel-rod bonded in glulam. The results of experimental data and numerical calculations proved that the transient temperature distrubutions are more complex than anticipated including pronounced temperature gradients along rod length. Thus more simple ideas of the temperature distributions (steel rod always in equilibrium with the surrounding air; wood as perfect isolating material) turned out to be too crude. So, temperature variations in the time domain of hours cause complex uneven temperature distributions in the regarded compound and hence eigenstrains and stresses. The latter aspect will be dealt with seperately.

REFERENCES

AICHER, S., HERR, J. (1998) *Investigations on high strength glulam framecorners with glued-in steel connectors.* Proceedings 5th World Conference on Timber Engineering, Vol. 1, pp. 273 - 280

AMSTUTZ, ED. (1955) *Über das Zusammenwirken von Beton und Bewehrung in Stahlbetonbauwerken.* Bauingenieur 10, pp.353 - 359

BATZER, H. (1985) *Polymere Werkstoffe*. Volume I, Georg Thieme Verlag Stuttgart. New York

BUCHANAN, A. H., TOWNSEND, P. K. (1998) *Portal frame knee joints with epoxied steel dowels.* Unpublished report, Canteprise, University of Canterbury, Christchurch

EHLBECK, J., BELCHIOR-GASPARD, P., GEROLD, M. (1992) *Eingeleimte Gewindestangen unter Axialbelastung bei Übertragung von großen Kräften und bei Aufnahme von Querzugkräften in Biegeträgern, Teil 2, Einfluß von Klimaeinwirkungen und Langzeitbelastung.* Versuchsanstalt für Stahl, Holz und Steine, Abteilung Ingenieurholzbau, Universität Karlsruhe

FAIRWEATHER, R. H. (1992) *Beam column connections for multistorey timber buildings.* Research Report 92/5, Department of Civil Engineering, University of Canterbury, Christchurch

GRÖBER, ERK, GRIGULL (1963) *Wärmeübertragung.* Springer, Berlin, Göttingen , Heidelberg

KOLLMANN F., (1982) *Technologie des Holzes und der Holzwerkstoffe.* Springer

N. N. (1990) *Konstruktionsklebstoffe, Araldit AW 106, Härter HV 953 U.* Ciba-Geigy AG, Publ. Nr. 24109/12/d

RIBERHOLT, H., (1986) *Glued bolts in glulam.* Department of Structural Engineering, Technical University of Denmark, Serie R, No.210, Lyngby